Evaluation of Microstructure and Texture of Alloy–90 Sheets

Alapati Venkateswarlu
Research Scholar, Bhagwant University, Ajmer, India

Prof. Dr.V.K Sharma
Vice Chancellor, Bhagwant University, Ajmer, India

Dr.L.Rama Krishna
Scientist-'E'
International Advanced Research Centre for powder Metallurgy and New Materials (ARCI),Hyderabad

Abstract - ALLOY–90 refers to a family of austenitic nickel-based super alloys. Nimonic alloys typically consist of roughly 80% nickel and 20% chromium with additives such as titanium and aluminium. The main use is in gas turbine blades. Nickel-based super alloys have been widely used in aircraft engines and land-based gas turbines where high strength at elevated temperatures is required. Improved properties may be achieved by modifying alloy chemistry and processing route. The high temperature strength of these alloys is not only a function of microstructural changes in the material, but the result of a competition between two deformation modes, i.e. the normal low to mid temperature tensile deformation and deformation via a creep mode. Nickel-based super alloys, among several high temperature structural alloys, are the prime materials for numerous advanced high temperature structural components. None of these studies have addressed the influence of microstructure and texture for ultra-thin sheet applications. Hence, a comprehensive study has been undertaken to evaluate the ambient temperature deformation characteristics as a function of degree of cold rolling and ageing.

Key words: Formability, Alloy 90, Impact

I. INTRODUCTION

ALLOY–90 refers to a family of austenitic nickel-based super alloys. Nimonic alloys typically consist of roughly 80% nickel and 20% chromium with additives such as titanium and aluminium. The main use is in gas turbine blades. Nickel-based super alloys have been widely used in aircraft engines and land-based gas turbines where high strength at elevated temperatures is required. Due to its ability to withstand very high temperatures, These alloys might be used in any environment that requires resistance to heat and corrosion but where the mechanical properties of the metal must be retained. Improved properties may be achieved by modifying alloy chemistry and processing route. The high temperature strength of these alloys is not only a function of microstructural changes in the material, but the result of a competition between two deformation modes, i.e. the normal low to mid temperature tensile deformation and deformation via a creep mode. Nickel-based super alloys, among several high temperature structural alloys, are the prime materials for numerous advanced high temperature structural components. In the past, a few attempts have been made to study the deformation behaviour of the Nimonic 90 alloy for sheet metal applications. However, these studies were limited to different commercial grades such as cold rolled sheets of thicknesses up to 2 mm. None of these studies have addressed the influence of microstructure and texture for ultra-thin sheet applications.

II. SCOPE OF THE WORK

Nickel based super alloys typically have austenitic face-centered cubic (fcc) crystal structure and hence, are expected to show low degrees of anisotropy (both in in-plane and through – thickness directions) in their mechanical properties. However, it is recently observed that some of the newer alloys such as Nimonic alloys exhibit considerable degree of anisotropy in mechanical propertied due to strong crystallographic texture, often develop due to cold working [1-4]. Such anisotropy of engineering materials manifests itself as a variation in the mechanical properties in different test directions and the same is important for the following reasons:

The Alloy-90, whose formability (drawability) is studied in the present investigation is a wrought nickel base super alloy and derives its strength from precipitation of fine, coherent γ' within fcc γ matrix. The alloy has excellent ambient and elevated temperature deformability with good welding characteristics. Nimonic 90 is a Nickel-Chromium-Cobalt alloy being precipitation hardenable, having high stress-rupture strength and creep resistance at high temperatures up to about 950°C (1740°F). It is widely used and a well proven alloy in high temperature conditions.

III. Chemical Composition of Alloy-90 (It describes the actual composition of alloy-90 and other alloys)

Alloy	Composition, in Wt. %												Nickel
	C	Si	Cu	Fe	Mn	Cr	Ti	Al	Co	Mo	B	Zr	
Nimonic 80A	0.04 0.10	1.0 max	0.2 max	1.0 max	1.0 max	18.0 21.0	1.8 2.7	1.0 1.8	2.0 max	0.3 max	0.0015 0.005	0.04 0.10	Bal.
Nimonic 81	0.05	0.5 max	0.2 max	1.0 max	0.5 max	30.0	1.8	0.9	2.0 max	0.3 max	0.002	0.06	Bal.
Alloy 90	**0.05 0.13**	**1.5 max**	**0.2 max**	**1.0 max**	**1.0 max**	**18.0 21.0**	**2.0 2.7**	**1.15 1.65**	**15.0 18.0**	**0.3 max**	**0.0015 0.005**	**0.04 0.10**	**Bal.**

Table.1

IV. Typical Properties of alloy 90

Table-2 it describes the Typical properties of Alloy-90 are covered in the following table.

Property	Metric	Imperial
Density	8.18 g/cm^3	0.296 lb/in^3
Melting point	1370 °C	2500 °F
Co-Efficient of Expansion	12.7 µm/m.°C (20-100 °C)	7.1x10^{-6} in/in.°F (70-212 °F)
Modulus of rigidity	82.5 kN/mm^2	11966 ksi
Modulus of elasticity	*213 kN/mm^2 **227 / 240 kN/mm^2	30894 ksi 32924 / 34810 ksi

* Solution Annealed + Aged **Spring Temper and Aged Table.2

Alloy-90 is widely used as cold rolled sheet product for a number of high temperature applications such as aircraft turbine and land-based-turbine engine components, due to its high creep strength and superior oxidation resistance. These applications include low-temperature combustors, transition liners and some ring components. However some of the recent applications of Alloy-90 sheet, especially the ultra thin sheets for thermal protection systems, need specific studies to evaluate in detail the factors that influences the cold rolling and drawability. Effect of ageing and in-plane anisotropy are the two most critical areas, which provide the scientific basis to this characterization. Such scientific study also acquires importance as the alloy 90 sheets are, till-date, not studied for their drawability characteristics. Hence, the present thesis addresses these issues in detail and the study is aimed at providing basic scientific inputs towards arriving at the solutions for alloy-90 alloy sheet for ultra thin sheet applications. The properties evaluated in the present thesis include tensile flow behaviour in various microstructural conditions such as Solution treated, aged for different times, apart from the microstructure as well as texture determination. The data obtained are analyzed for anisotropy in tensile properties (strength and ductility) and yield behaviour. The tensile properties were determined in five different test directions, namely P (Longitudinal Direction i.e. parallel to the rolling direction), P+30º, P+45º,P+60º and P+90º (perpendicular to the rolling direction). These data as a function of ageing and sheet thickness along with the details of microstructure and texture, when evaluated, analyzed and obtained the relevant yield properties, have become valuable and essential data inputs for the principal aim of the thesis, i.e. the numerical simulation of formability in general, drawability characteristics in particular.

V. Evolution of Research in methods of Drawing:

5.1 Deep drawing, even though is one of the most basic processes in sheet metal working, it involves very complicated deformation mechanics. The numerical difficulty in the finite element analysis of the deep drawing processes arises due to the existence of compressive stress in the sheet plane and the occurrence of unloading. The drawing load increases with the punch displacement. As the punch moves, the flange part of the sheet is drawn into the die cavity. The punch load decreases after a critical point because less resisting force to drawing is developed in the flange. In the range of decreasing punch load, unloading occurs at the wall of a drawn cup. Therefore, in analyzing the bending-dominant processes like deep drawing, the effect of unloading should also be considered. The state of stress at the wall and at the flange is basically tensile stress in axial or radial direction and compressive stress in the circumferential direction. As the sheet metal has relatively a small dimension in the thickness direction, the compressive stress may cause wrinkling in the actual process or numerical buckling in simulation. The numerical buckling is the mesh buckling phenomenon occurring in the finite element analysis at the region of high compressive stress like actual buckling.

5.2 Yield Behaviour: The yield behaviour and the characteristics that influence the yield behaviour in several structural materials have been the subjects of scientific studies for sheet metal applications. Recent studies have also attempted to correlate the microstructure, texture, in-plane anisotropy in yield stress and work hardening exponent to the deep drawability. However such studies required to be conducted in case of the Nimonic 90 alloy as this particular alloy has been the prime candidate material chosen for ultra-thin sheet applications for honeycomb structures of thermal protection systems. Nickel based super alloys typically have axi-symmetric face-centered cubic (fcc) crystal structure and hence, are expected to be isotropic. Studies have been reported in the literature in which these symmetric crystal structured alloys are found to exhibit high degree of isotropy in their tensile deformation [3, 4]. However, some of the recent studies revealed especially those on Al-Li alloys (though they too are of fcc crystal structure) have exhibited considerable degree of anisotropy in mechanical properties due to strong crystallographic texture, often developed due to extensive cold working [2,4]. Similarly, the ageing conditions too affect the yield behavior and also anisotropy in the yielding significantly [2]. Such an anisotropy of engineering materials manifests itself as a variation in the mechanical properties in different test directions and the same is important for the following reasons: (a) directionality in the properties may be utilized to obtain improved formability; (b) service performance of a material in a particular orientation may be selectively improved and most importantly, (c) components may become susceptible to failure in an unfavorable direction, with catastrophic consequences. Both the aspects of yield behavior and the anisotropy can be studied by evaluating the tensile properties in various in-plane directions, namely the longitudinal (L, along the rolling direction) and 30°, 45° and 60° to the rolling direction, designated as L+30°, L+45° and L+60°, respectively as well as long – transverse (LT, perpendicular to the rolling direction). Alternatively, the yield behavior can also be studied by determining the yield loci using asymmetrical Knoop microhardness indenter. These aspects in case of the Nimonic 90 sheet material are not studied in detail till date and hence, are the subject of present study. In the present study, we report the tensile deformation behavior, anisotropy in tensile properties and yield loci in addition to the microstructural and textural effects on the observed deformation behavior.

5.3 Transient flow behavior: The prominent objective of the present study is that the alloy in solution treated condition exhibit transient flow behavior at lower strain. Such behavior has been reported earlier in several FCC materials with low stacking fault energy such as α-brass, silver and austenitic stainless steels. Ludwigson suggested that the transient flow at low strains i.e., at the onset of plastic deformation, in low stacking materials is associated with planar glide and leads to the formation of cell structure causing a change in macroscopic flow behavior above a certain critical strain known as transient strain.

The stainless steels and 70-30 brass, with the lowest stacking fault energies exhibit the smallest negative values of n2 and the largest values of transient strain, εL (8-15 %). Metals with somewhat higher stacking fault energies, namely copper and silver, exhibit more negative values of n2 and lower values of εL (3%). Aluminium and nickel, with the highest stacking fault energies in this series obey the Hollomon relation and do not exhibit any transition in flow behaviour.

VI. Affect of Specimen Orientation

The other aspect to be investigated in the present study is the affect of specimen orientation with respect to rolling direction on strain hardening behavior of the alloy. Strain hardening rate, θ (=$d\sigma/d\varepsilon$) versus strain plots for the alloy in solution treated as well as aged conditions and for different specimen orientations. while the alloy specimen with longitudinal orientation (i.e., parallel to rolling direction), exhibit marginally highest strain hardening rates, specimen with long transverse orientation exhibits lowest strain hardening rate both in solution treated and aged conditions. However, for all other orientations (i.e., A+30º, A+45º and A+60º), the strain hardening rate data is fairly very close and lie in between those of longitudinal and Longitudinal Transverse orientations. Such a behavior is consistent with the in-plane anisotropy, with regard to tensile properties.

VII. Material model and properties of tooling

In the present study, an effort will be made to comprehensively evaluate and rationalize the in-plane anisotropy and the effect of ageing on the nature of deformation (strain hardening behaviour) and formability characteristics, especially the limit drawing ratio and forming limit diagram. Despite weak crystallographic texture and excellent ductility and high work hardening exponents, the alloy sheet alloy-90 exhibits significant extent of in-plane anisotropy in its tensile properties and yield loci. The of microstructural features, mainly such as precipitation of □' strengthening phase obtainable by ageing after cold rolling and solutionizing, was found not to alter the nature of deformation significantly. However the alloy in aged condition shows reduced degree of anisotropy with significantly improved strength characteristics and moderate decrease in drawability. The alloy under tensile deformation exhibits mixed nature of fracture, comprising of a predominant ductile microdimpled fracture with minor degree of transgranular shear fracture. Transmission electron microscopy (TEM) will be used to examine the specimens to record the microstructural characteristics at significantly higher magnifications. These characteristics include the nature (size and shape), distribution of strengthening precipitates and the carbide particles with or without the details of composition.

VIII. CHEMICAL COMPOSITION OF THE EXPERIMENTAL ALLOY SHEET (TABLE-3 DESCRIBES THE MODIFIED COMPOSITION OF ALLOY-90 SHEETS)

I. Element	C	Co	Cr	Mo	Al	Si	Ti	Mn	B	P	Ni
Actual Composition, (wt. %) - 1.0 mm thick sheet 0.5 mm thick sheet	0.058 0.053	15.03 15.36	18.65 18.90	0.28 0.295	1.55 1.34	1.45 1.05	2.10 2.04	0.42 0.43	0.001 0.095	0.005 0.005	Bal. Bal
Specified composition	0.05-0.13	15-18	18-21	0.3-max	1.15-1.65	1.5-max	2.0-2.7	1.0-max	0.0015 0.005	--	Bal.

Table -3

IX. RESEARCH METHODOLOGY

The as-received material will be in the form of cold rolled and solution treated sheets of thicknesses 1 mm and 0.5 mm. The cold rolled sheets will be solution treated at 1150±10º C for 5-15 mins., followed by air cooling. The present work aims at comprehensive evaluation of monotonic tensile deformation, work hardening and drawability characteristics of Nimonic alloy 90 sheet. The data obtained from the monotonic tensile tests are integrally used to determine the drawability characteristics. Transmission electron microscopy (TEM) will be used to examine the specimens to record the microstructural characteristics at significantly higher magnifications

The evaluation of anisotropy requires the determination of properties in various test directions. The number of directions to be tested depends upon the product type, such as plate, sheet, extrusion, forging and castings. Mechanical properties are generally evaluated in three orthogonal directions namely,

a. The longitudinal direction (where the stress axis is parallel to the direction of rolling, forging etc. and designated as P in deformation studies),
b. The long transverse direction (where the stress axis is perpendicular to the direction of rolling, forging etc and lies in the plane of rolling, forging etc designated as P+90º in deformation studies) and
c. The short transverse direction (where the stress axis is along the thickness direction of the product and designated as SL or ST in deformation studies).
d. For plate and sheet products, the properties in the other in-plane directions, such as P+30º, P+45º,P+60º and P+90º (where specimen stress axis is at 30°, 45°, 60°and 90° to the rolling direction), also become important.

The properties evaluated in the present work include tensile flow behaviour in various microstructural conditions such as Solution treated, aged for different times, apart from the microstructure as well as texture determination. The data obtained will be analyzed for anisotropy in tensile properties (strength and ductility) and yield behaviour. The tensile properties will be determined in five different test directions, namely P,P+30º, P+45º,P+60º and P+90º. These data as a function of ageing and sheet thickness along with the details of microstructure and texture, when evaluated, analyzed and obtained the relevant yield properties, will become valuable and essential data inputs for the principal aim of the present work, i.e. the numerical simulation of formability in general, drawability characteristics in particular.

X. RESULTS

The alloy sheet in the as-received, i.e., solution treated and cold rolled condition was further subjected to aging treatment at 1110 K in a vacuum furnace for different durations. Specimens for microstructure (both optical and transmission electron microscopy), and texture evaluation, Vicker's hardness and tensile property evaluation are withdrawn from the vacuum heat treatment furnace after appropriate duration of ageing treatment. The specimens were then processed further. Based on the aging curve (variation of Vickers macro hardness with aging time), determined and shown in Fig.1, tensile properties were evaluated on specimens from 0.5 and 1mm thick alloy sheets that were aged at this temperature for select durations of 1, 8 and 20 hours.

The effect of ageing is discussed in terms of variation in hardness (Vickers hardness number obtained using 10 Kg load) for different ageing conditions as well as sheet thicknesses. Such variation describes the ageing behaviour qualitatively as the time intervals are relatively larger. In both sheet thicknesses the hardness increases significantly within 1 hour ageing at 1110 K. Such an increase is significantly higher for thinner sheet of 0.5 mm thickness. Further ageing to 8h increases the hardness marginally (Fig. I and Table -4). Further increase in ageing time decreases the hardness significantly. The hardness values obtained on specimens aged to 20h show a decrease in hardness values that are up to 20% lower as compared the 8h aged condition, depending upon sheet thickness. Hence, the present nimonic alloy attains peak hardness at 8h ageing, which is designated as peak aged condition. Limited tensile tests conducted as a function of ageing too reveal similar trends. Such tensile data are included in Table .3 for the sake of comparison

(Table-4 describes the Vickers hardness and Yield stress values of alloy 90 sheet in cold rolled + Solution treated and different aged Conditions of 1mm and 0.5mm thickness.)

Condition	Vickers hardness number$_{10}$		Yield Stress (MPa) at $\dot{\varepsilon} = 10^{-4}\ S^{-1}$	
	1 mm	0.5 mm	1 mm	0.5 mm
Initial	260	290	548	689
1110 K / 1 hr	335	373	795	875
1110 K / 8 hr	349	405	835	980
1110 K / 20 hr	331	339	748	819

Table 4

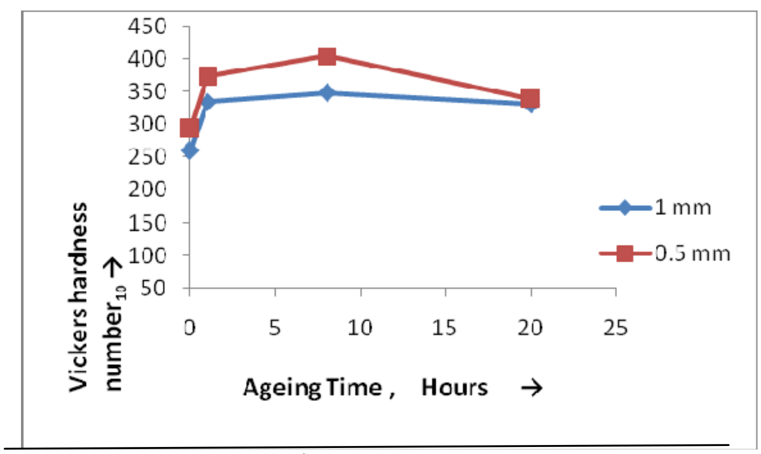

Fig-I

10.1. Results of Optical microscopy

Cold rolled and Solution treated condition: The samples to be examined for optical microscopy were first mounted in Bakelite and then polished using different grades of emery

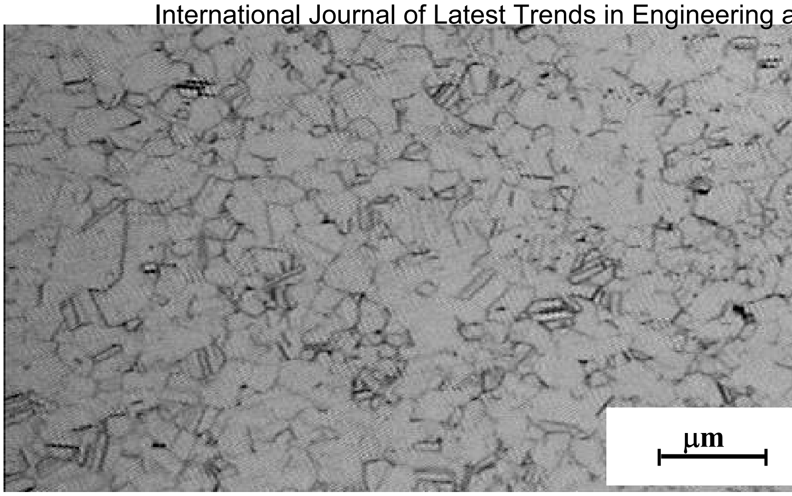

Fig-II.: Micrograph of alloy 90sheets in the as-received cold rolled + solution treated condition.

paper beginning with a coarse (100 grit SiC paper) and finishing with a fine size (600 grit SiC paper). After preliminary polishing, the samples were final polished on the cloth using diamond paste. The samples were then thoroughly cleaned using ultrasonic container, half-filled with acetone. The cleaned samples were subsequently etched using an etchant consisting of 15 % sulphuric acid, 5%nitric acid, 15% phosphoric acid and balance water. Fig-II shows the microstructure of the alloy sheet in the as-received solution treated condition. Though large number of specimens were examined, the alloy's microstructure was found to be quite uniform and it principally consists of partially recrystallized, equi-axed grains in sheet surface and unrecrystallised grains in sheet thickness direction with high density of annealing twins. The average grain size is approximately 30 □m in the surface direction.

The microstructure obtained from the specimens of alloy sheets of two thicknesses in the peak aged condition found to be almost of the same features (within the same variation as in solution treated + Cold Rolled condition) at the optical level and hence are not reported separately.

10.2. Results of Transmission electron microscopy (TEM)

Transmission electron microscopy was used to examine the specimens to record the micro structural characteristics at significantly higher magnifications. These characteristics include the nature (size and shape), distribution of strengthening precipitates and the carbide particles with or without the details of composition. The samples for TEM were thinned by polishing using various grades of emery paper to a thickness of 100 μm. The samples were then further thinned using the twin jet polishing technique with an electrolyte of mixed acids (lactic acid- 10%, sulphuric acid - 7%, nitric acid - 3%, hydro fluoric acid - 2% and methanol - balance, by volume). The conditions employed for thinning were – 30 oC and 25 V. The thinned foils were examined in EM 430 T and JEOL transmission electron microscopes.

Transmission electron micrographs, given in Figs. III.3 – III.5 show the finer micro structural details of the alloy sheet of 1mm thickness in the as-received, i.e, solution treated and cold rolled condition (The features are similar for 0.5mm thick sheet). The TEM bright field micrograph (Fig. III.3a) and the corresponding selected area diffraction pattern (Fig. III.3b) show that the matrix of the present Nimonic sheet does not contain any detectable levels of strengthening precipitates in the Solution Treated condition. However, the alloy sheet does exhibit the presence of reasonable high density of dislocations (Fig. III.3c).

The alloy sheet in the solution treated condition was found to contain significant amounts of two kinds of carbide particles. The first set of the carbides (Fig. III.4) are cubic in shape and have a definite face centered cubic (FCC) crystal structure with an average lattice parameter of 4.37 A°. These carbide particles have an average size of 80 nm. The second type of carbide particles that are found to be present in the alloy sheet in the ST condition (Fig. III.5a) are angular in shape and are relatively coarser (average size is 160-180 nm) as compared to the first set of carbides. The selected area diffraction pattern obtained shows that these carbide particles (Fig. III.5a) too have FCC crystals structure with an average lattice parameter of 4.36 A°.

The energy dispersive X-ray spectrum (EDXS) obtained from these carbide particles (Fig. III.5a) clearly shows that the carbides contain Ti and Mo elements as major constituents. The analysis of chemical composition and crystal structure indicate that these particles could be of MC type, i.e., [(Ti,Mo)C]. Further, a small increase in the observed lattice parameter of 4.36 A° as compared to reported theoretical lattice parameter of TiC particles (4.3178 A°) clearly indicates that these MC type carbide particles contain significant amounts of Mo in the Ti lattice sites of the FCC crystal.

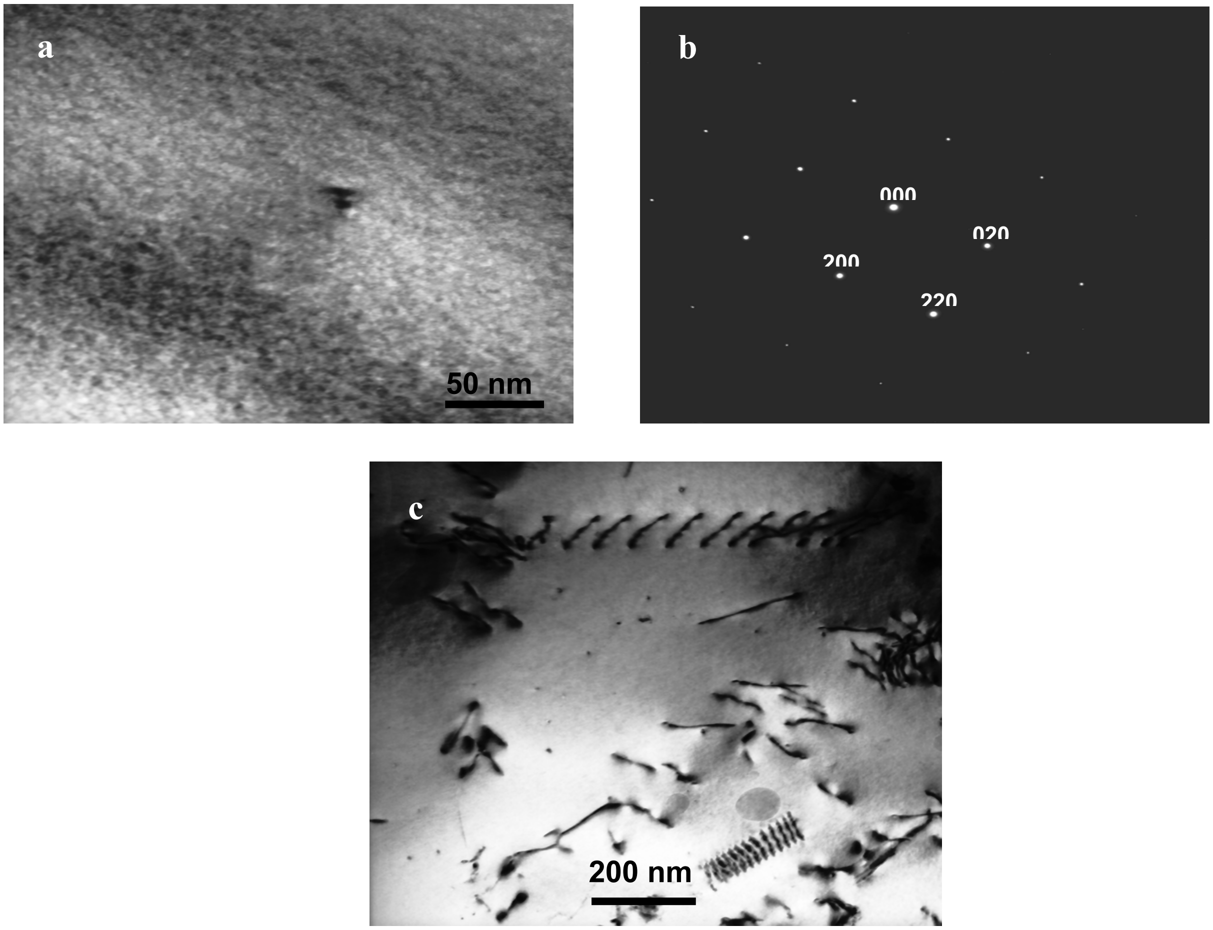

Fig. III.3: (a) TEM bright field image showing matrix structure in <100> orientation.
(b) Selected area electron diffraction pattern matrix. The diffraction pattern indicates the absence of ’ phase. (c) TEM bright field image showing dislocation substructure observed in the matrix

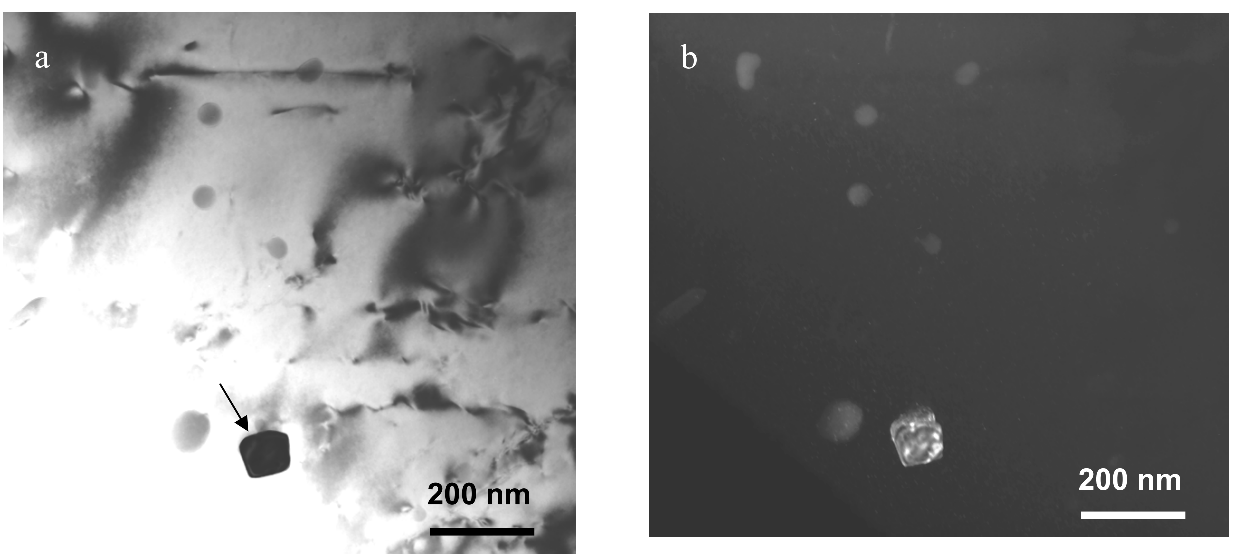

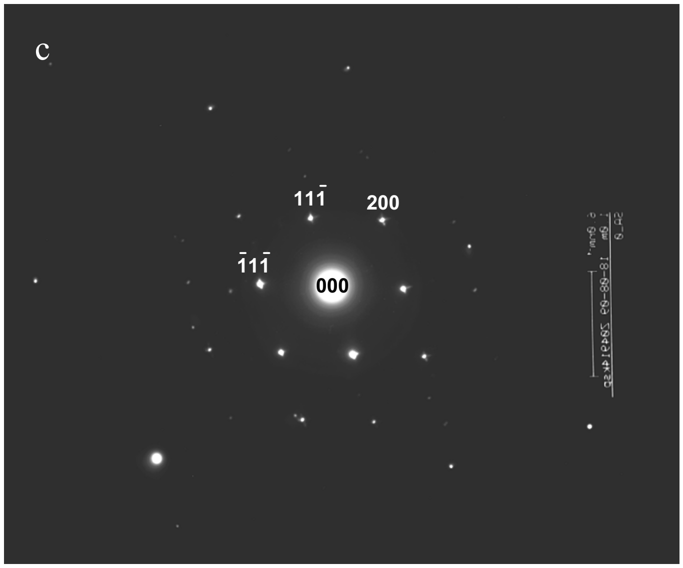

Fig. III.4: (a) and (b) TEM bright field and dark field images showing carbide particles respectively. (c) Selected area electron diffraction pattern obtained form the carbide particle [arrow marked in (a)], representing [011] zone axis of the FCC crystal structure, with an average lattice parameter ao = 4.37 A°.

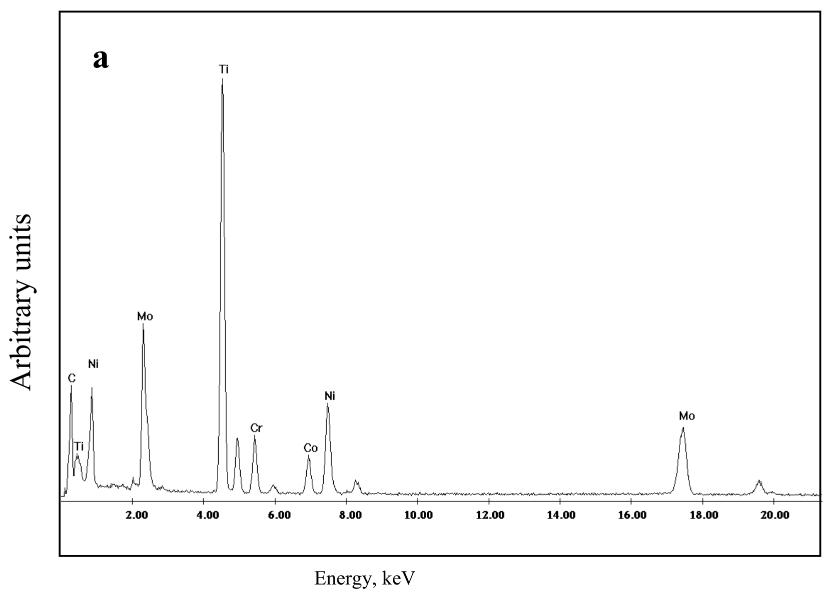

Fig. III.5: (a) Energy dispersive X-ray spectrum collected from the particle indicating that the carbide contains Ti and Mo as major elements. The chemical composition and crystal structure indicates that these carbide particles could be of MC type [(Ti,Mo)C]. The theoretical lattice parameter of TiC is 4.3178 A°. The small increase in lattice parameter can be attributed to the induction of Mo into the TiC.

The studies conducted on the optical micrography of the aged specimens of the alloy sheet reveal no observable diffraction in the microstructures that is shown in Fig. III.2. However, at the higher magnification obtainable by transmission electron micrography, the alloy sheet in the 8h aged condition was found to contain large volume fraction of uniformly distributed □’ precipitates (Fig. III.6).

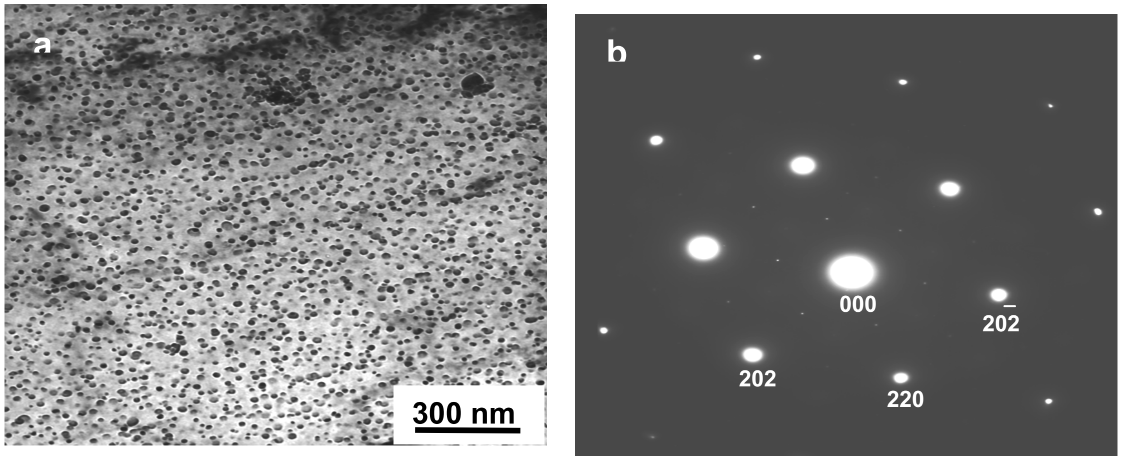

Fig. III.6: (a) TEM bright field image showing □’ precipitates in <111> and <100> of matrix orientations respectively after ageing at 1110K/8h. (b) Selected area electron diffraction patterns corresponds to Fig. (a). The super lattice reflection in the diffraction patterns corresponding to □’ precipitates in the matrix.

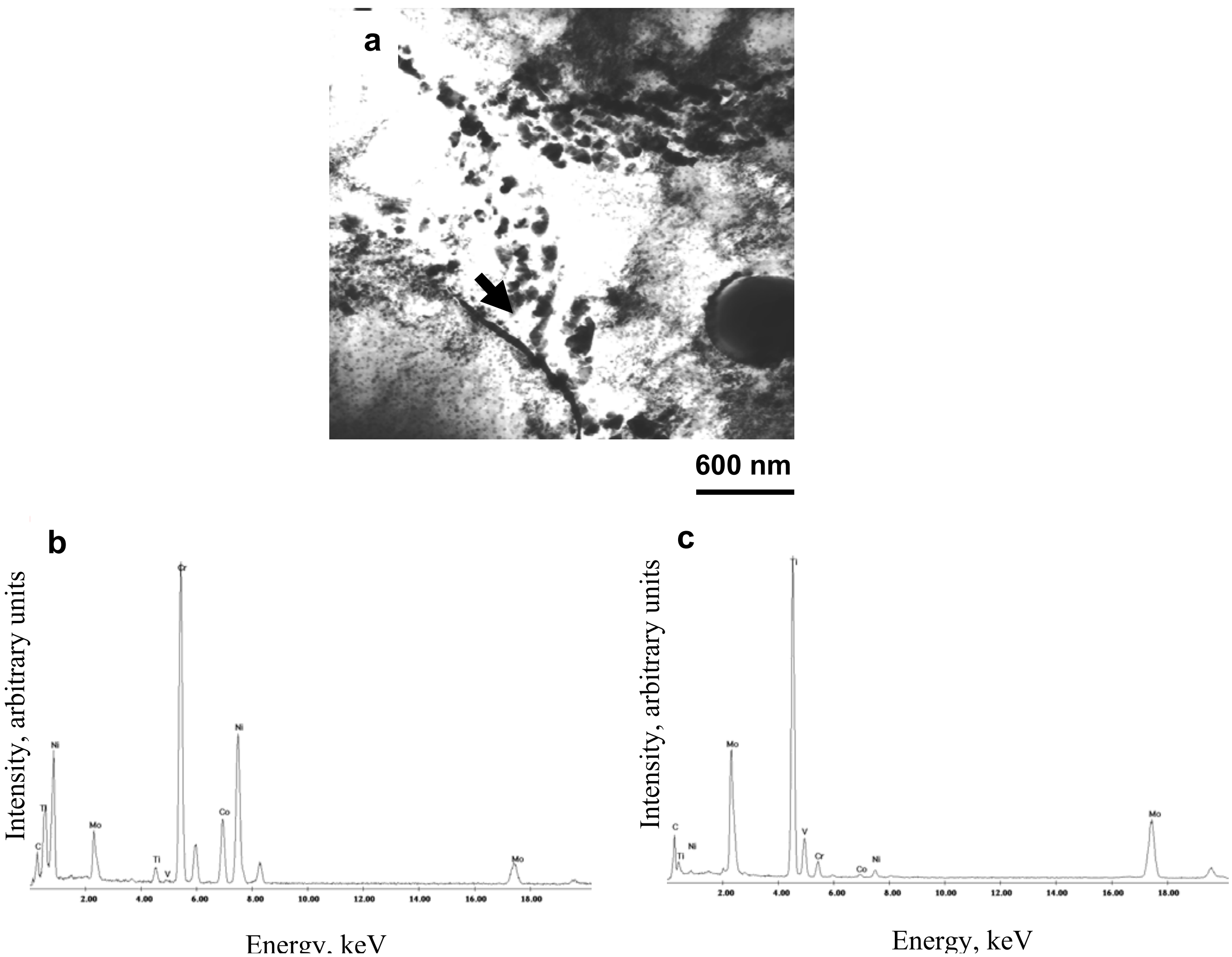

Fig. III.7: (a) TEM bright field images showing $M_{23}C_6$ type carbides at the grain boundaries and twin boundaries, respectively. MC type carbide (arrow marked in Fig. (a)) also observed in the matrix, which is similar to that observed in the as solution treated condition.(c) Energy Dispersive X-ray Spectrum (EDXS) obtained from the grain boundary precipitates showing Cr enrichment. (c) EDXS obtained from the MC type particle (arrow marked in Fig. (a)) in the matrix showing Ti enrichment.

The TEM bright field micrography in the two matrix crystal orientations of <111> and <100> (Fig. III.6 a and c) clearly show that the □’ precipitates are spherical in shape and are in the size range of 20-30 nm. A comparison of the selected area diffraction (SAD) patterns obtained from these □’ precipitates in <111> and <100> matrix crystallographic orientations (Fig. III.6 b and d respectively). With these reported for □’ precipitates clearly show a one-to-one correspondence, confirming that the strengthening that occurs in the present nimonic alloy is primarily due to the □’ precipitates. The presence of jointly appearing super lattice reflections (appearing as in a circular fashion around the central 000 diffraction spot and the 202, 220 and 202 diffraction spots in Fig. III.6 (b) and (d) clearly indicate that the □’ precipitates are highly coherent and ordered.

Just as in cold rolled + solution treated condition, the alloy sheet in 8h aged condition too reveals the presence MC type carbides with Ti enrichment. These carbides are arrow marked in Fig. III.7 (a) and appear to be significantly coarser 1-500 nm and spherical as compared to those in the solution treated condition (see the MC carbides in Fig. III.5). Further, the alloy sheet in the aged condition found to posses significantly larger amounts of M23C6 type of carbides along in the grain and twin boundaries (Fig. III.7 a). These finer carbide particles were observed through EDXS (Fig. III.7 b) is found to be Cr – enriched in contrast to the Ti – enrichment in the coarser MC carbides (Fig. III.7 c).

XI. CONCLUSION

Finally The finite element simulation of drawability characteristics, namely limit drawing ratio and forming limit diagram of alloy 90 using the explicit dynamic analysis code LSDYNA, will be evaluated and reported. The selection of finite element model, material models (blank, punch and die) and the properties required for the numerical simulation will be described. Numerical simulations are carried out iteratively to find out the limit strains of the Nimonic 90 alloy sheet of 1 mm thickness in peak aged conditions and forming limit curves are determined. Finally, the procedure is validated with the analytical formulae developed using vertex theory.

REFERENCES

[1] Singh AK, Saha GG, Gokhale AA and Ray RK, Evolution of texture and microstructure in a thermo-mechanically processed Al-Li-Cu-Mg alloy, Metall. Mater. Trans. A, Vol. 29A (1998) pp. 665-675.

[2] Howard-White FB, Nickel- An historical review, VanNostrand, Princeton, (1963).

[3] Donachie MJ, Superalloys, American Society for Metals (1984).

[4] Sims CT, Stoloff NS and Hagel WC, Superalloys II, John Willey and Sons, New York, (1987).

[5] McLean M, Webster GA, Nabarro FRN and Cottrel A, Nickel based Superalloys: Current status and potential, Phil. Trans. Royal Soc. London, Vol. 351 (1995) pp. 419-43

[6] Joseph R. Davis, S. L. Semiatin, ASM Metals Handbook, Forming and Forging, ASM International, 9th edition, Vol. 14 (1989) pp. 891-892.

[7] Kotthaus H, An investigation of transportability of test results from models to full scale tooling for deep drawing of round scaled components, Dr. Ing. Thesis, Technishe Hochschule, Stuttgart (1955).

[8] Made W and Deh R, Deep-drawing tests and failure of soft, unalloyed steels, Manufacturing Technology, Vol. 17 (1967) pp. 665-672.

[9] Koelzer H, The behavior of deep drawing sheets as a function of testing methods, Dr.Ing thesis, Technishe Hochule, Braunschwig, (1979).

[10] Ludwigson DG, Modified stress-strain relation for F.C.C. metals and alloys, Metall. Trans., Vol. 2 (1971) pp. 2825-2828.

[11] Sivaprasad PV, Venugopal S and Venkadesan S, Work hardening behaviour of the Ni-Fe based superalloy IN718, Metallurgica and Materials Trans. A, Vol. 28A (1997) pp. 171-178.

[12] Kuo VWC and Starke EA, The development of two texture variants and their effect on the mechanical behavior of a high strength P/M aluminium alloy, Metall. Trans. A, Vol. 16A (1985) pp. 1089-1103.

[13] Jata KV, Panchandeeswaran S and Vasudevan AK, Evolution of texture, microstructure and mechanical property anisotropy in an Al-Li-Cu alloy, Material Science Engineering, Vol. A257 (1998) pp. 37-46.